Weierstraß-Institut
für Angewandte Analysis und Stochastik

Leibniz-Institut im Forschungsverbund Berlin e. V.

Preprint ISSN 2198-5855

Unipolar drift-diffusion simulation of S-shaped current-voltage relations for organic semiconductor devices

Jürgen Fuhrmann[1], Duy Hai Doan[2], Annegret Glitzky[1], Matthias Liero[1], Grigor Nika[1]

submitted: December 18, 2019

[1] Weierstrass Institute
Mohrenstraße 39
10117 Berlin
Germany
E-Mail: juergen.fuhrmann@wias-berlin.de
annegret.glitzky@wias-berlin.de
matthias.liero@wias-berlin.de
grigor.nika@wias-berlin.de

[2] m4sim GmbH
Seydelstraße 31
10117 Berlin
Germany
E-Mail: duyhai.doan@m4sim.de

No. 2660
Berlin 2019

2010 *Mathematics Subject Classification.* 65M08, 35J92, 80M12, 80A20.

Key words and phrases. Non-isothermal drift-diffusion, organic semiconductors, finite volumes, generalized Scharfetter–Gummel scheme, path following.

The authors gratefully acknowledge the funding by the German Research Foundation (DFG) under Germany's Excellence Strategy – The Berlin Mathematics Research Center MATH+ (EXC-2046/1, project ID: 390685689) in project AA2-1 and AA2-6.

Edited by
Weierstraß-Institut für Angewandte Analysis und Stochastik (WIAS)
Leibniz-Institut im Forschungsverbund Berlin e. V.
Mohrenstraße 39
10117 Berlin
Germany

Fax: +49 30 20372-303
E-Mail: preprint@wias-berlin.de
World Wide Web: http://www.wias-berlin.de/

Unipolar drift-diffusion simulation of S-shaped current-voltage relations for organic semiconductor devices

Jürgen Fuhrmann, Duy Hai Doan, Annegret Glitzky, Matthias Liero, Grigor Nika

Abstract

We discretize a unipolar electrothermal drift-diffusion model for organic semiconductor devices with Gauss–Fermi statistics and charge carrier mobilities having positive temperature feedback. We apply temperature dependent Ohmic contact boundary conditions for the electrostatic potential and use a finite volume based generalized Scharfetter-Gummel scheme. Applying path-following techniques we demonstrate that the model exhibits S-shaped current-voltage curves with regions of negative differential resistance, only recently observed experimentally.

1 Introduction

The temperature activated hopping transport of charge carriers in organic semiconductors results in a strong interplay between electric current and heat flow. It gives rize to interesting phenomena like S-shaped Current-Voltage (CV) relations with regions of negative differential resistance in Organic Light Emitting Diodes (OLEDs) [12] or leads to inhomogeneous luminance in large-area OLEDs. Moreover, electrothermal effects influence the performance of transistors [10].

As demonstrated in [12], p-Laplace thermistor models that describe the total current and heat flow in a device, are able to capture the positive temperature feedback in OLEDs. Especially, they can reproduce experimentally observed S-shaped CV-relations and inhomogeneous current density and temperature distributions in large-area OLEDs. But, details such as separate electron and hole current flow, generation-recombination and related heat productions, as well as energy barriers at material interfaces cannot be included.

In this paper, we present a numerical approximation of an electrothermal drift-diffusion model for organic semiconductor devices and study its ability to reproduce S-shaped CV-relations. For simplicity, for this proof of concept we use vertically layered device structures.

2 Electrothermal Drift-Diffusion Description of Organic Semiconductor Devices

We restrict our considerations to the unipolar (n-doped) case, for the full model see [3]. Then the electrothermal behavior is described in a drift-diffusion setting by PDEs for the electrostatic potential ψ, the electrochemical potential φ_n, and the temperature T. In the device domain Ω we consider the stationary coupled system

$$\begin{aligned} &-\nabla\cdot(\varepsilon\nabla\psi) = q(C-n),\\ &-\nabla\cdot j_n = 0, \quad j_n = -qn\mu_n\nabla\varphi_n,\\ &-\nabla\cdot(\lambda\nabla T) = qn\mu_n|\nabla\varphi_n|^2 =: H. \end{aligned} \tag{2.1}$$

This system results from the coupling of a generalized, unipolar van Roosbroeck system and a heat flow equation that includes the Joule heating as heat source. The dielectric permittivity is denoted by $\varepsilon = \varepsilon_0\varepsilon_r$, q is the elementary charge, C represents the doping density, and λ is the thermal conductivity.

DOI 10.20347/WIAS.PREPRINT.2660 Berlin 2019

Additionally we take into account the specialities of organic semiconductors, namely i) the statistical relation between chemical potential and charge carrier density is given by Gauss–Fermi integrals leading to bounded charge carrier densities and ii) a mobility function μ_n depending on temperature, density, and electric field strength. The mobility laws are fitted from a numerical solution of the master equation for the hopping transport in a disordered energy landscape with a Gaussian density of states [11]. The charge carrier density n in (2.1) is given by

$$n = N_{n0}(T)G\Big(\frac{q(\psi-\varphi_n)-E_L(T)}{k_{\mathrm{B}}T};\frac{\sigma_n(T)}{k_{\mathrm{B}}T}\Big), \tag{2.2}$$

where k_{B} is Boltzmann's constant. We assume that the parameters E_L (lowest unoccupied molecular orbital level), σ_n^2 (its variance), and N_{n0} (total density of transport states) are only weakly temperature dependent such that we neglect this weak temperature dependence in our investigations. We set

$$\eta_n = \eta_n(\psi,\varphi_n,T) := \frac{q(\psi-\varphi_n)-E_L}{k_{\mathrm{B}}T}, \quad s_n = s_n(\sigma_n,T) := \frac{\sigma_n}{k_{\mathrm{B}}T}.$$

The function $G : \mathbb{R}\times[0,\infty)\to(0,1)$ is defined by the Gauss–Fermi integral

$$G(\eta_n,s_n) := \frac{1}{\sqrt{2\pi}}\int_{-\infty}^{\infty}\exp\left(-\frac{\xi^2}{2}\right)\frac{1}{\exp\left(s_n\xi-\eta_n\right)+1}\,\mathrm{d}\xi.$$

According to [11], the mobility $\mu_n = \mu_n(T,n,|\nabla\psi|)$ is a temperature, density and electric field strength dependent function of the form

$$\mu_n(T,n,F) = \mu_{n0}(T)\times g_1(n,T)\times g_2(F,T), \quad \mu_{n0}(T) = \mu_{n0}c_1\exp\left\{-c_2s_n^2\right\}. \tag{2.3}$$

For the considerations of our paper we set $g_1 = g_2 \equiv 1$ and take only the positive temperature feedback μ_{n0} into account. System (2.1), (2.2) is closed by mixed boundary conditions for the drift-diffusion system combined with Robin boundary conditions for the heat flow equation modeling a heat sink with fixed temperature T_a.

In [9] the solvability of the bipolar system including the full mobility functions (weak solutions of continuity equations and Poisson equation, entropy solution of the heat flow equation) is established.

In the non-isothermal case, the modeling of (ideal) Ohmic contacts requires local charge neutrality at the contact for the actual temperature dependent state (ψ,φ_n,T). For an applied voltage V, this leads to the nonlinear relation at the contacts $\Gamma_{D_i}\subset\partial\Omega$ for the prescribed value $\psi_0 = \psi - V$:

$$C_{D_i}(\psi;V,T) := C - N_{n0}G\Big(\frac{q(\psi-V)-E_L}{k_{\mathrm{B}}T};\frac{\sigma_n}{k_{\mathrm{B}}T}\Big) = 0. \tag{2.4}$$

A straightforward generalization of the computational approach for the isothermal case would result in the necessity to update ψ_0 for each modification of the temperature T, leading to an additional iterative loop for the determination of each bias solution. To avoid this iteration, we use (2.4) directly as a nonlinear Dirichlet boundary condition for the electrostatic potential ψ depending on T and treat it with the nonlinear solver along with all other nonlinearities.

3 Discretization Scheme

We use a finite volume method and partition the computational domain Ω by a Voronoi mesh with m Voronoi volumes $\{V_l\}_{l=1,\dots,m}$ and accompanying collocation points $\{x_l\}$. The potentials ψ, φ_n, and the temperature T are evaluated at each node x_l. The discretized system corresponding to (2.1) is derived by integrating the equations over each Voronoi volume V_l, applying Gauss's theorem, and then suitably approximating the boundary and volume integrals. We also add the subscript l in all quantities to denote their corresponding numerical values at x_l. In what follows, we will assume that the material parameters ε, μ_{n0}, N_{n0}, and λ are constant, otherwise, suitable averages have to be used.

The resulting surface integrals are split into two parts: integrals over interfaces between two adjacent Voronoi boxes and integrals over boundary parts of the device:

$$\int_{\partial V_l} -\varepsilon\nabla\psi\cdot\nu \,\mathrm{d}\Gamma = \sum_{V_r\in\mathcal{N}(V_l)} \int_{\partial V_l\cap\partial V_r} -\varepsilon\nabla\psi\cdot\nu \,\mathrm{d}\Gamma + \int_{\partial V_l\cap\partial\Omega} -\varepsilon\nabla\psi\cdot\nu \,\mathrm{d}\Gamma,$$
$$\int_{\partial V_l} -j_n\cdot\nu \,\mathrm{d}\Gamma = \sum_{V_r\in\mathcal{N}(V_l)} \int_{\partial V_l\cap\partial V_r} -j_n\cdot\nu \,\mathrm{d}\Gamma + \int_{\partial V_l\cap\partial\Omega} -j_n\cdot\nu \,\mathrm{d}\Gamma,$$
$$\int_{\partial V_l} -\lambda\nabla T\cdot\nu \,\mathrm{d}\Gamma = \sum_{V_r\in\mathcal{N}(V_l)} \int_{\partial V_l\cap\partial V_r} -\lambda\nabla T\cdot\nu \,\mathrm{d}\Gamma + \int_{\partial V_l\cap\partial\Omega} -\lambda\nabla T\cdot\nu \,\mathrm{d}\Gamma.$$

Here $\mathcal{N}(V_l)$ stands for the set of Voronoi volumes V_r which are adjacent to the Voronoi volume V_l. The integrals over interfaces $\partial V_l\cap\partial V_r$ must be treated specifically in order to maintain the consistency of the numerical solution, whereas the surface integrals over $\partial V_l\cap\partial\Omega$ are evaluated by quadrature rules after replacing the normal flux in the integrand by the corresponding boundary condition.

Numerical fluxes through interfaces $\boldsymbol{\partial V_l\cap\partial V_r}$. Whereas the integrals of $-\varepsilon\nabla\psi\cdot\nu$ and $-\lambda\nabla T\cdot\nu$ over the interface $\partial V_r\cap\partial V_l$ are approximated by the conventional finite difference approximations

$$\int_{\partial V_r\cap\partial V_l} -\varepsilon\nabla\psi\cdot\nu \,\mathrm{d}\Gamma \approx \frac{\mathrm{mes}\,(\partial V_r\cap\partial V_l)}{|x_l-x_r|}\varepsilon\,(\psi_l-\psi_r)$$

(similarly for $-\lambda\nabla T\cdot\nu$), the corresponding integrals in the continuity equations require some extra effort

$$\int_{\partial V_r\cap\partial V_l} j_n\cdot\nu \,\mathrm{d}\Gamma \approx \frac{\mathrm{mes}\,(\partial V_r\cap\partial V_l)}{|x_l-x_r|}J_n^{l;r},$$

where the numerical fluxes $J_n^{l;r}$ are determined by a modification of the Scharfetter-Gummel scheme based on averaging of inverse activity coefficients introduced in [6] and discussed with respect to degenerate semiconductors in [5, 4]. We introduce some notation for the definition of the expressions $J_n^{l;r}$:

$$\psi_{l,r} := \frac{\psi_l+\psi_r}{2},\ \varphi_{n;l,r} := \frac{\varphi_{n;l}+\varphi_{n;r}}{2},\ T_{l,r} := \frac{T_l+T_r}{2},\ U_T^{l,r} := \frac{k_\mathrm{B}T_{l,r}}{q},\ s_n^{l,r} := \frac{\sigma_n}{k_\mathrm{B}T_{l,r}},$$
$$\overline{\eta}_{n;l} := \eta_n\,(\psi_l,\varphi_{n;l},T_{l,r})\,,\ \overline{\eta}_{n;r} := \eta_n\,(\psi_r,\varphi_{n;r},T_{l,r})\,,\ \overline{\eta}_n^{l,r} := \eta_n\,(\psi_{l,r},\varphi_{n;l,r},T_{l,r})\,,$$
$$n^{l,r} := N_{n0}G\left(\overline{\eta}_n^{l,r};s_n^{l,r}\right),\ \mu_n^{l,r} := \mu_{n0}\,(T_{l,r})\,.$$

With the above definitions and the Bernoulli function, $B(x) = \frac{x}{\exp(x)-1}$, the numerical fluxes $J_n^{l;r}$ have the form

$$J_n^{l;r} = -qN_{n0}\mu_n^{l,r}U_T^{l,r}\frac{G\left(\overline{\eta}_n^{l,r};s_n^{l,r}\right)}{\exp\left(\overline{\eta}_n^{l,r}\right)}\left[\mathrm{e}^{\overline{\eta}_{n;l}}B\left(\frac{\psi_l-\psi_r}{U_T^{l,r}}\right)-\mathrm{e}^{\overline{\eta}_{n;r}}B\left(-\frac{\psi_l-\psi_r}{U_T^{l,r}}\right)\right].$$

For the discretization of the full bipolar model taking into account the complete mobility functions from organics including the factors g_1 and g_2 we refer to [3].

Numerical treatment of the boundary conditions on $\boldsymbol{\partial V_l\cap\partial\Omega}$. The realization of no-flux and Robin boundary conditions is based on the evaluation of the corresponding surface integrals by a midpoint quadrature rule. Dirichlet boundary conditions are implemented using the Dirichlet penalty method: We replace the Dirichlet boundary conditions for φ_n by $j_n\cdot\nu+\Pi(\varphi_n-V)=0$, and treat them like Robin boundary conditions. The penalty parameter Π is a large number which results in marginalizing the normal flux contributions. In order to approximate the nonlinear Dirichlet boundary condition (2.4), we use a similar idea. We replace (2.4) by $-\varepsilon\nabla\psi+\Pi C_{D_i}(\psi;V,T)=0$ and treat the resulting boundary condition as a nonlinear Robin boundary condition. Using this approach, the nonlinearity (2.4) can be treated without any additional iteration along with all the

other nonlinearities in the resulting system of equations by the general Newton solver coupled to a parameter embedding scheme.

Volume integrals. Whereas for the integral of the charge density $C - n$ we use the midpoint rule, the integral of the Joule heat H is approximated using the fluxes $J_n^{l;r}$,

$$\begin{aligned} &\int_{V_l} (C-n)\,\mathrm{d}x \approx \mathrm{mes}\,(V_l)\,(C_l - n_l), \\ &\int_{V_l} H\,\mathrm{d}x \approx \sum_{V_r \in \mathcal{N}(V_l)} \frac{\mathrm{mes}\,(\partial V_l \cap \partial V_r)}{2\mathrm{dim}\,(\Omega)}\, J_n^{l;r}\,(\varphi_{n;l} - \varphi_{n;r})\,. \end{aligned} \tag{3.1}$$

Here, we followed the idea proposed in [1] and exploited in [7] allowing to evaluate the Joule heating approximation for electrons and holes by edge contributions.

Path-following method for calculation of S-shaped CV-curves. For a device with two Dirichlet boundary parts Γ_{D_1} and Γ_{D_2}, where on Γ_{D_2} the potential is set to zero and on Γ_{D_1} to the (spatially constant) externally applied voltage V, we determine the CV-relation by calculating the current over Γ_{D_1}. Since organic semiconductors show a pronounced electrothermal feedback that can lead to S-shaped CV-relations, a voltage controlled simulation is unable to cover the full characteristic, since at the lower turning point of the S-curve one would not find a point on the curve with increased voltage and only slightly increased current and related temperature, see e.g. Fig. 1 a). For such voltage values, only points on the upper branch of the S-curve are available, related to very different current and temperature values. In other words, for increasing voltage, if at all the method would converge, one could only jump to the upper part of the S-curve and the (unstable) region of negative differential resistance of the S-curve is impossible to resolve. Therefore we implemented a path-following method to trace the S-curve. With the discrete equations for all Voronoi boxes $\{V_l\}$ we arrive at a system of $3m$ coupled nonlinear algebraic equations for $u = (\psi_l, \varphi_{n;l}, T_l)_{l=1,\dots,m}$ of the form $F(u, V) = 0$, $F : \mathbb{R}^{3m} \times \mathbb{R} \to \mathbb{R}^{3m}$. We adapt the technique described in [7, Sec. 5] which was used in [12] to simulate S-shaped CV-relations for organic LEDs resulting from an electrothermal modeling by p-Laplace thermistor models to the drift-diffusion setting.

4 Simulation Results

The finite volume method has been implemented in the prototype semiconductor device simulator ddfermi [2] which is based on the PDE solution toolbox pdelib [8].

We give a proof of concept that electrothermal drift-diffusion models from Sec. 2 can exhibit S-shaped CV-relations and restrict our simulations to a 340 nm thick, uniformly n-doped layer that is contacted by two metal layers. Due to the high conductivity of the metal layers we assume that the potential is constant here and neglect the metal layer entirely. Instead, we prescribe Dirichlet boundary conditions on the parts Γ_{D_1} and Γ_{D_2}. On Γ_{D_2} the potential is set to zero and on Γ_{D_1} to the externally applied voltage V. We determine the CV-relation of the organic device by calculating the current over Γ_{D_1}. We found a parameter range leading to a pronounced occurrence of S-shaped CV-relations. The used parameters are collected in Table 1.

Table 1: Simulation parameters

parameter	value	parameter	value	parameter	value
ε	$4.0\,\varepsilon_0$	E_H	0.0 eV	N_{n0}	$10^{21}\,\mathrm{cm}^{-3}$
λ	$0.4\,\mathrm{Wm}^{-1}\mathrm{K}^{-1}$	T_a	220 K	μ_{n0}	$0.8\,\mathrm{cm}^2\mathrm{V}^{-1}\mathrm{s}^{-1}$
κ	$10^3 \dots 10^5\,\mathrm{Wm}^{-2}\mathrm{K}^{-1}$	c_1	1.0	doping	$5 \cdot 10^{18}\,\mathrm{cm}^{-3}$
σ_n	$0.05 \dots 0.08$ eV	c_2	0.4	thickness	340 nm

To discuss the phenomenon of S-shaped CV-relations and their appearance in dependence on physical parameters, we present two types of parameter variations. In Fig. 1 a), b) we study the influence of the disorder

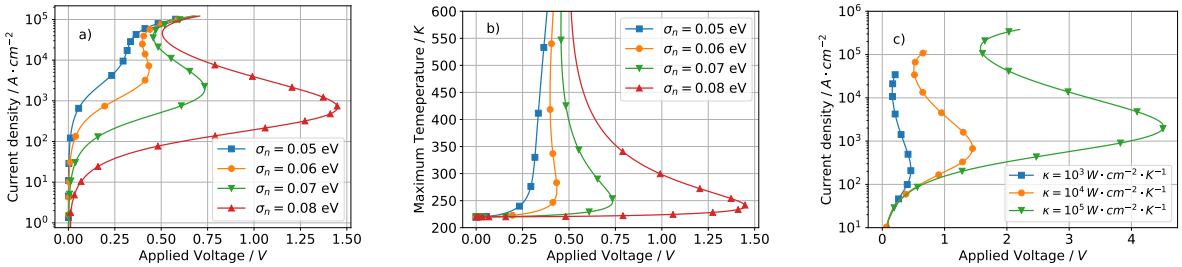

Figure 1: CV-characteristics using the electrothermal drift-diffusion model for different disorder parameters σ_n (Fig. a)), Fig. b) shows the resulting maximal temperature in the device for $\kappa = 10^4$ W/(m^{2}K). Fig. c) depicts CV-curves for different thermal outcoupling regimes and $\sigma_n = 0.08$ eV

parameter σ_n on the electrothermal interaction in the device. The resulting CV-relations are depicted in Fig. 1 a), Fig. 1 b) shows the maximal device temperature over the applied voltage. Whereas for $\sigma_n = 0.05$ eV no S-shaped CV-relation occurs, although such behavior evolves for higher σ_n. With increasing σ_n the first turning point of the curve moves to a higher applied voltage but the related current density decreases and the 'S' becomes more pronounced. Fig. 1 c) contains CV-relations for a variation of the thermal outcoupling conditions realized by Robin boundary conditions of the form $\lambda \nabla T \cdot \nu + \kappa(T - T_a) = 0$ on $\partial\Omega$ for different values of κ. Better cooling broadens the 'S', for the two turning points the applied voltage as well as the current density increase. The exemplary variations of physical parameters show that the complex nonlinear interplay leads to strong variations in the shape of the CV-characteristics.

5 Conclusion and Remarks

We presented a discretization scheme for the electrothermal drift-diffusion model (2.1) for organic semiconductor devices. We formulated temperature dependent nonlinear Dirichlet boundary conditions for the electrostatic potential (2.4) at Ohmic contacts, which take into account the shift of the equilibrium potential due to changing device temperature.

We used a finite volume based generalized Scharfetter-Gummel scheme implemented in the prototype semiconductor device simulator `ddfermi` [2] on top of the PDE solver toolbox pdelib [8]. Via a path-following technique, we demonstrated that the model and its discretization for certain parameters exhibit the phenomenon of an S-shaped CV-relation with regions of negative differential resistance. The ability to simulate S-shaped CV-relations using drift-diffusion type electrothermal models is to our knowledge a novelty. Although CV-relations have been observed experimentally in [12], there is a need to be properly modeled in order to understand and optimize the device behavior.

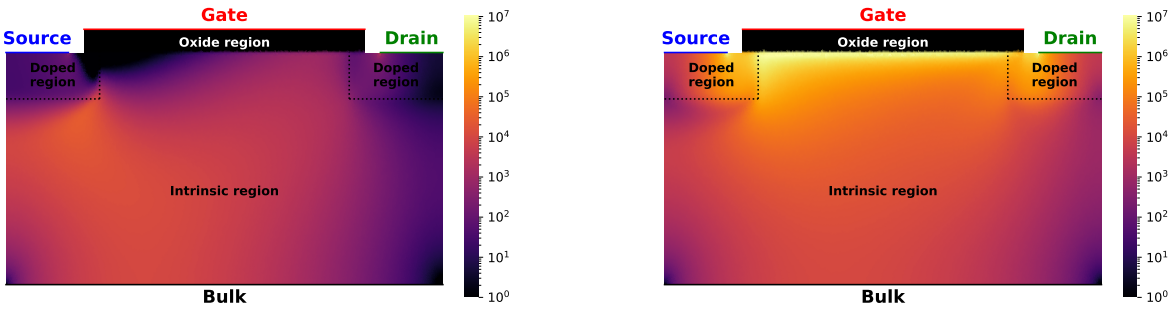

Figure 2: Simulated Joule heat densities [W/cm^3] (source terms in the heat flow equation) in an organic transistor that demonstrate the change of the electrothermal regime when opening the channel by increasing the gate voltage from 0V (left) to 1V (right) for a fixed source-drain voltage of 1V.

Besides device characteristics, our model (2.1) and its discretization are capable to describe the spatially resolved electrothermal behavior of real 3D organic semiconductor devices in terms of charge carrier densities, current densities, potentials, temperature distributions. Fig. 2 compares the produced Joule heat densities for an organic thin-film transistor with fixed source-drain voltage of 1V when the channel is opened by raising the gate voltage from 0V (left) to 1V (right).

Simulations for real organic device structures and realistic physical parameters help to estimate the region of a stable working regime guaranteeing the absence of material destruction due to overheating. Furthermore, the description of the spatially resolved electrothermal behavior of real devices is very important for understanding the effect of thermal switching, device degradation, device breakdown and local heating (hot spots) in large area devices.

References

[1] A. Bradji and R. Herbin, *Discretization of coupled heat and electrical diffusion problems by finite-element and finite-volume methods*, IMA J. Numer. Anal. **28** (2008), 469–495.

[2] D. H. Doan, P. Farrell, J. Fuhrmann, M. Kantner, Th. Koprucki, and N. Rotundo, *ddfermi – a drift-diffusion simulation tool*, 2019, URL: http://doi.org/10.20347/WIAS.SOFTWARE.DDFERMI.

[3] D. H. Doan, A. Fischer, J. Fuhrmann, A. Glitzky, and M. Liero, *Drift-diffusion simulation of S-shaped current-voltage relations for organic semiconductor devices*, WIAS-Preprint 2630, Berlin, 2019.

[4] P. Farrell, Th. Koprucki, and J. Fuhrmann, *Computational and analytical comparison of flux discretizations for the semiconductor device equations beyond Boltzmann statistics*, Journal of Computational Physics **346** (2017), 497–513.

[5] P. Farrell, N. Rotundo, D.H. Doan, M. Kantner, J. Fuhrmann, and T. Koprucki, *Drift-diffusion models*, Handbook of Optoelectronic Device Modeling and Simulation, chap. 50 (J. Piprek, ed.), vol. 2, CRC Press Taylor & Francis, 2017, pp. 733–771.

[6] J. Fuhrmann, *Comparison and numerical treatment of generalised Nernst–Planck models*, Computer Physics Communications **196** (2015), 166–178.

[7] J. Fuhrmann, A. Glitzky, and M. Liero, *Hybrid finite-volume/finite-element schemes for $p(x)$-Laplace thermistor models*, Finite Volumes for Complex Applications VIII - Hyperbolic, Elliptic and Parabolic Problems: FVCA 8, Lille, France, June 2017 (C. Cancès and P. Omnes, eds.), Springer International Publishing, Cham, 2017, pp. 397–405.

[8] J. Fuhrmann, H. Langmach, M. Liero, T. Streckenbach, and M. Uhle, *pdelib – FVM and FEM toolbox for partial differential equations*, 2019, URL: http://pdelib.org.

[9] A. Glitzky, M. Liero, and G. Nika, *An existence result for a class of electrothermal drift-diffusion models with Gauss–Fermi statistics for organic semiconductor devices*, WIAS-Preprint 2593, Berlin, 2019.

[10] M. P. Klinger, A. Fischer, H. Kleemann, and K. Leo, *Non-linear self-heating in organic transistors reaching high power densities*, Scientific Reports **8** (2018), 9806.

[11] P. Kordt, P. Bobbert, R. Coehoorn, F. May, C. Lennartz, and D. Andrienko, *Organic Light Emitting diodes*, Handbook of Optoelectronic Device Modeling and Simulation, chap. 15 (J. Piprek, ed.), vol. 1, CRC Press Taylor & Francis, 2017, pp. 473–522.

[12] M. Liero, J. Fuhrmann, A. Glitzky, T. Koprucki, A. Fischer, and S. Reineke, *3D electrothermal simulations of organic LEDs showing negative differential resistance*, Opt. Quantum Electron. **49** (2017), 330/1–330/8.